

Article

A Novel Nanoplatfrom Based on Biofunctionalized MNPs@UCNPs for Sensitive and Rapid Detection of *Shigella*

Yaqi Song, Min Chen, Zhongyu Yan, Lu Han, Leiqing Pan  and Kang Tu 

College of Food Science and Technology, Nanjing Agricultural University, Nanjing 210095, China

* Correspondence: kangtu@njau.edu.cn; Tel.: +86-25-8439-9016

Abstract: *Shigella*, a typical and fatal foodborne pathogen with strong infectivity and survivability in foodstuff, demands a simple and sensitive detecting method. In this study, we reported a novel nanoplatfrom based on biofunctionalized magnetic nanoparticles (MNPs) modified upconversion nanoparticles (UCNPs) for rapid and specific determination of *Shigella*. Due to base pairing, *Shigella* aptamer-functionalized horseradish peroxidase (HRP) combined with complementary strand-modified MNPs@UCNPs. In the absence of *Shigella*, HRP associated with MNPs@UCNPs were magnetically separated, and colorless 3,3',5,5'-tetramethylbenzidine (TMB) was oxidized into blue oxTMB. The overlap between oxTMB's absorption peak and MNPs@UCNPs' emission peak caused the fluorescence quenching at 545 nm. The MNPs@UCNPs fluorescence biosensor was achieved to detect *Shigella* in 1 h, with a limit of detection of 32 CFU/mL. This work showed a rapid and specific sensing platform and produced satisfactory chicken sample results.

Keywords: upconversion nanoparticles; Fe₃O₄; TMB; fluorescence; *Shigella*



Citation: Song, Y.; Chen, M.; Yan, Z.; Han, L.; Pan, L.; Tu, K. A Novel Nanoplatfrom Based on Biofunctionalized MNPs@UCNPs for Sensitive and Rapid Detection of *Shigella*. *Chemosensors* **2023**, *11*, 309. <https://doi.org/10.3390/chemosensors11050309>

Academic Editor: Ambra Giannetti

Received: 10 April 2023

Revised: 8 May 2023

Accepted: 17 May 2023

Published: 20 May 2023



Copyright: © 2023 by the authors. Licensee MDPI, Basel, Switzerland. This article is an open access article distributed under the terms and conditions of the Creative Commons Attribution (CC BY) license (<https://creativecommons.org/licenses/by/4.0/>).

1. Introduction

Foodborne diseases are a broad spectrum of illnesses and a significant cause of morbidity and mortality worldwide, associated with bacteria, viruses, parasites, as well as bio-toxins derived from food. In today's interconnected and interdependent world, local foodborne disease outbreaks have become a potential threat to the globe. According to the federal government in the US, there are approximately 48 million cases of foodborne diseases annually, with an estimated 128,000 hospitalizations and 3000 deaths [1].

Bacteria are the most common cause of foodborne illnesses and widely exist in a variety of types and properties [2]. Among substantial foodborne pathogenic bacteria, *Shigella* is a highly contagious pathogen with a rare infectious dose of about 10 to 100 organisms that cause illnesses such as nausea, vomiting, diarrhea, and even sepsis [3]. Therefore, it is essential to monitor *Shigella* and routinely analyze it in the food supply chain for food safety, clinical diagnosis, as well as treatment.

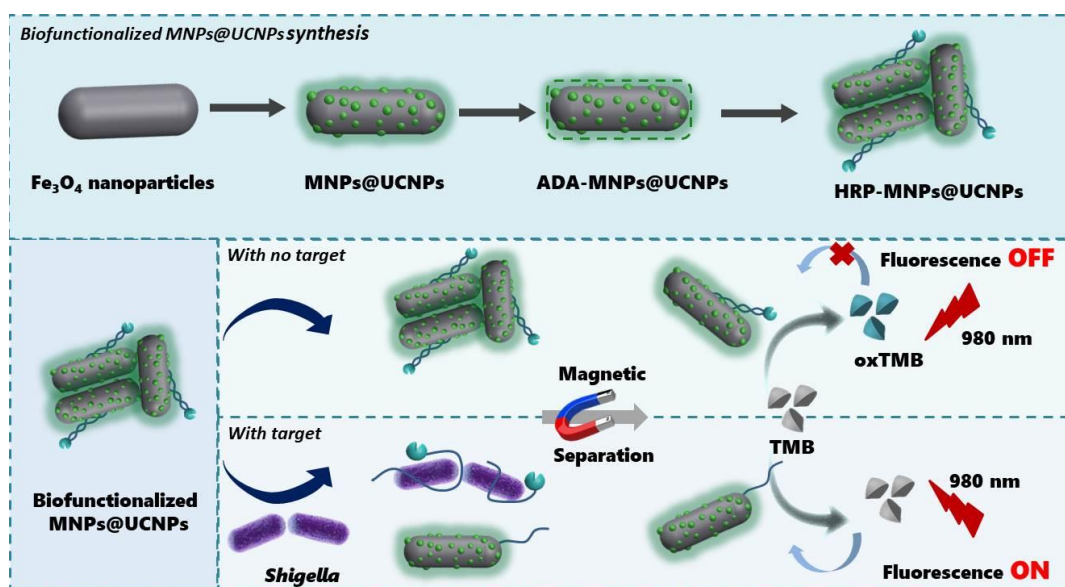
The conventional strategies for foodborne pathogen determination are mainly based on culturing and the plate-counting method, which was considered the gold standard for bacteria analysis, the nucleic acid amplification technique, as well as enzyme-linked immunosorbent assay (ELISA) [4]. Culturing and plate counting usually take a long time to gain a confirmed consequence [5]. Nucleic acid amplification obtains highly sensitive detection results while suffering from high cost, expensive equipment, as well as complicated pretreatment steps [6,7]. ELISA is a sensitive and specific detection method to quantify substances, while it still has limitations such as tedious procedure, sample matrix interference, and temporary readouts [8]. These traditional methods are associated with time-consuming, complicated operations and high-cost instruments. Therefore, it is urgent to develop a rapid, sensitive, and low-cost approach to *Shigella* determination.

Over the years, biosensors based on nanomaterials have been a research hotspot in hazardous substance detection due to their simplicity, rapidity, and cost-effectiveness [9].

The biosensors can be divided into colorimetric, fluorescent, Raman scattering spectroscopic, and electrochemical sensors [10]. Among these biosensors, fluorescence biosensors have received more and more attention for foodborne pathogen assays due to their high sensitivity, low cost, and short response time. Unfortunately, conventional fluorescence biosensors generally use fluorescent dyes [11] and quantum dots (QDs) [12] as fluorescence reagents, which still suffer from a couple of limitations, including narrow excitation spectrum, short fluorescence lifetime, susceptibility to photobleaching, and unstable optical properties [13,14]. Compared to these fluorescence donors, upconversion nanoparticles (UCNPs), as a new type of fluorescence material, possess more stable optical properties, longer fluorescence lifetime, less toxicity, and are less prone to photobleaching [15]. Recently, a couple of strategies based on UCNPs have been applied to food safety monitoring, including foodborne bacteria, heavy metals, antibiotics, and pesticide residues [16–19]. In addition, some novel UCNPs fluorescence biosensors have been developed for foodborne hazardous substances in foodstuff. For example, the UCNPs fluorescence nanoprobe-based fluorescence resonance energy transfer (FRET) was constructed for *Shigella* detection with a low detection limit of 30 CFU/mL [20]. Ouyang et al. fabricated a UCNPs-MnO₂ luminescent resonance energy transfer (LRET) biosensor for carbendazim pesticide in food with high sensitivity (0.05 ng/mL) [21]. Shao et al. established an “off-on” FRET probe based on UCNPs for Cu²⁺ assay with high sensitivity (18.2 nM) and excellent recovery (96–108%) [22]. Therefore, there are broad prospects to fabricate a fluorescence biosensor based on UCNPs to develop the biological assay field.

Although fluorescence biosensors based on UCNPs possess superiority in food safety monitoring, the target enrichment and matrix influence are still unsolved issues in biosensors construction [23]. Magnetic nanoparticles (MNPs) have been widely applied to the separation and enrichment of foodborne pathogens in foodstuff and received so far attention due to easy synthesis and modification, high stability, and convenient operation [24]. The ferrite colloid of magnetite (Fe₃O₄) is a major type of MNPs and has gained increasing interest in microbiological detection due to biocompatibility [25]. Narges et al. built a nanobiosensor based on gold and magnetic nanoparticles for *Shigella* species detection with a low detection limit of 10² CFU/mL [26]. Shi et al. increased enrichment efficiency of *Staphylococcus aureus* via Fe₃O₄ MNPs, and the limit of detection was found to be 10³ CFU/mL combined with PCR [27]. Multifunctional MNPs@UCNPs possess the characteristics of fluorescence and magnetism, which improve accuracy and reliability, eliminate the interference of foodstuff, as well as simplify procedures [23]. Nevertheless, there are few reports on the detection of *Shigella* by multifunctional MNPs@UCNPs. Thus, there remain substantial chances for the fabrication of simple, effective, and sensitive fluorescence biosensors based on multifunctional MNPs@UCNPs.

Novel biofunctionalized MNPs@UCNPs connected with HRP by noncovalent forces between *Shigella* aptamer and the complementary strand were designed in this study. Scheme 1 displays the process of the proposed fluorescence biosensor for *Shigella* detection. The MNPs@UCNPs were fabricated by a facile hydrothermal method and possessed both magnetic and fluorescent properties. The complementary strand-linked MNPs@UCNPs combined with *Shigella* aptamer-modified HRP due to base pairing. With the absence of *Shigella*, MNPs@UCNPs-modified HRP were magnetically separated so that the TMB was oxidized from colorless into blue, resulting in fluorescence quenching. The study covered the following points: (1) synthesis and characterization of MNPs@UCNPs; (2) fabrication and assessment of the detection system to determine *Shigella*; (3) specificity of the proposed nanoplatform based on biofunctionalized MNPs@UCNPs; (4) the application of the proposed method for *Shigella* detection in chicken. On the basis of adequate enrichment, unique UCNPs fluorescence emission, and strong quenching properties, the proposed fluorescence biosensor is able to determine *Shigella* with highly sensitive and precise results, providing a potential application in foodborne pathogens detection.



Scheme 1. Schematic presentation of the nanoplatform based on biofunctionalized MNPs@UCNPs for *Shigella* detecting.

2. Materials and Methods

2.1. Materials and Chemicals

Rare earth nitrates were obtained from Sigma-Aldrich. 1-octadecene, oleic acid, alendronic acid, CHCl_3 , HCl , NH_4F , NaOH , FeCl_3 , 1, 6-hexadiazine, and anhydrous sodium acetate were purchased from Alfa Aesar (Shanghai, China). 3-3',5,5'-tetramethylbenzidine horseradish peroxidase color development solution (P0209-100 mL) was purchased from Beyotime Biotechnology Co., Ltd. (Shanghai, China). The *Shigella*-specific aptamer and complementary strand were provided by Sango Biotechnology Co., Ltd. (Shanghai, China) with the sequence 5'-Biotin-CCG GAC TAG GGC TGG TTA GCT TCA ATA CTG CTG GGC GAG G-3' (apt1) and 5'- NH_2 -GGC CTG ATC CCG ACC AAT CGA AGT TAT GAC CCG CTC C-3' (apt2) [28]. Nanjing Agricultural University provided all foodborne pathogens involved in this study.

2.2. Synthesis and Modification of Fe_3O_4

According to a previous study, the monodisperse MNPs were synthesized [29]. Firstly, 1.1 g of FeCl_3 and 0.12 g of iron powder were added into 8 mL of dodecylamine and 3.5 mL of oleic acid. After the substance was dispersed completely, the mixed solution was transferred into a polytetrafluoroethylene-lined autoclave and heated to 190 °C for 6 h. Then, the autoclave was cooled to room temperature. The samples were separated and washed with ethanol and cyclohexane three times to remove unreacted precursors. Finally, the products were dried in a vacuum oven at 60 °C overnight.

2.3. Synthesis and Modification of MNPs@UCNPs

The MNPs@UCNPs were fabricated and modified with alendronic acid (ADA) following the reported method [30]. Firstly, 2 mL of Fe_3O_4 NPs (25 mg/mL) were added into 10 mL of DI water and 30 mL of 1-propanol under stirring at 25 °C for 30 min. $\text{RE}(\text{NO}_3)_3$ (RE = Y (78.5%), Yb (20%), Er (1.5%)), and 9 mmol NaF were introduced into the above solution under ultrasonic agitation. Then, 20 mL of EDTA solution (0.05 mmol/mL) were added to the flask. After a reaction for 30 min, the mixed solution was transferred into a polytetrafluoroethylene-lined autoclave and heated to 120 °C for 24 h. The samples were separated and washed with ethanol and DI water three times to remove nonmagnetic particles. Finally, the products were dried in a vacuum oven at 60 °C overnight.

Alendronic acid (ADA) was adopted for the water-soluble modification of UCNPs [31]. Initially, 5 mg of ADA and 20 mg of MNPs@UCNPs were dissolved in 0.4 mL of ethanol, 1 mL of CHCl_3 , and 0.6 mL of deionized water by ultrasound for 30 min. Then, the completely dissolved solution was pH adjusted to 2–3 by HCl (1 mol/L) and stirred for 1 h. Lastly, the products were dried in a vacuum oven after washing them with ethanol and deionized water (1:1 v/v).

ADA-UCNPs and *Shigella* aptamer conjugates were fabricated by a reported method with a slight modification [32]. Firstly, 10 mg of ADA-MNPs@UCNPs were dispersed into 5 mL of PBS buffer (pH = 7.2) and 1.25 mL of glutaraldehyde under stirring. After the reaction for 2 h, the MNPs@UCNPs were washed with PBS buffer (pH = 7.2) three times. Subsequently, 500 μL of *Shigella* aptamer (0.1 mmol/mL) were introduced into the above solution under shaking for 4 h. Finally; the MNPs@UCNPs and aptamer conjugates were washed several times by PBS buffer (pH = 7.2).

2.4. Microbial Culture

Shigella (ATCC 12022), *Salmonella typhimurium* (ATCC 14028), *Listeria monocytogenes* (ATCC 19111), *Staphylococcus aureus* (ATCC 130), *Pseudomonas aeruginosa* (ATCC 27853), *Escherichia coli* (ATCC 43889), and *Streptococcus thermophile* (ATCC 03872) were cultured in Luria–Bertani (LB) on a shaking incubator at 200 rpm at 37 °C overnight. The concentration of *Shigella* cells was calculated by the plate count method when the OD_{600} of bacterial cultures achieved 0.3.

2.5. Procedures for *Shigella* Fluorescent Detection

To access the sensitivity of the biofunctionalized MNPs@UCNPs fluorescence biosensor, a series of tenfold-diluted concentrations (10^8 CFU/mL–10 CFU/mL) of *Shigella* were determined by the proposed method. Firstly, 200 μL of streptavidin—HRP (0.02 mg/mL) were added into 50 μL of *Shigella* aptamer modified with biotin (10 mg/mL). Then, the above solution was mixed with 500 μL of MNPs@UCNPs to obtain the biofunctionalized MNPs@UCNPs connected with HRP. The *Shigella* of different concentrations (250 μL) was mixed with the above solution and incubated for 23 min at 37 °C. Then, the substance was magnetically separated and dispersed into 150 μL of PBS buffer (pH = 7.2). Subsequently, 350 μL of TMB horseradish peroxidase color development solution were added to the above solution and continued to incubate for 24 min. Finally, the fluorescence intensity at $\lambda_{\text{em}} = 545$ nm was recorded when the excitation laser was at 980 nm.

2.6. Specificity Analysis for *Shigella*

To complete the specificity tests of the proposed method, *Shigella* (ATCC 12022), *Salmonella typhimurium* (ATCC 14028), *Listeria monocytogenes* (ATCC 19111), *Staphylococcus aureus* (ATCC 130), *Pseudomonas aeruginosa* (ATCC 27853), *Escherichia coli* (ATCC 43889), and *Streptococcus thermophile* (ATCC 03872) at a concentration of 10^8 CFU/mL were determined by the biofunctionalized MNPs@UCNPs fluorescence sensor. The fluorescence intensity of different pathogens was measured for further comparison.

2.7. Detection of *Shigella* in Chicken Sample

To evaluate the developed method's potential application value and accuracy, we determined *Shigella* (ATCC 12022) in chicken breast meat. The artificially contaminated chicken samples were processed in the following steps [33]. Firstly, the chicken breast samples bought from the local supermarket were washed with saline and sterilized with 30 W ultraviolet for 30 min. Then, the sterilized chicken samples (25 g) were mixed with 250 mL of DI water and homogenized. Subsequently, the chicken samples were allowed to stand for 30 min to remove large particles and filtered through a 0.45 μm filtration membrane to reserve supernatant. Finally, *Shigella* in concentrations of 10^3 CFU/mL, 10^4 CFU/mL, and 10^5 CFU/mL were spiked into homogeneous supernatant. The fluorescence intensity of different concentrations of *Shigella* was measured to calculate the recovery.

3. Results

3.1. Characterization

A series of properties have been characterized, including morphology, size, crystal form, and surface groups, as depicted in Figure 1. Figure 1A,B reveal that the shape and size of MNPs@UCNPs had no noticeable difference after ADA modification. Moreover, it could be clearly observed that a mass of UCNPs was decorated on rod-shaped Fe_3O_4 NPs. The size of MNPs@UCNPs was about 320 nm in length and 160 nm in width, while the size of UCNPs was about 15 nm. Additionally, the crystal form of hexagonal-shaped UCNPs demonstrated that all peaks were in good agreement with the $\beta\text{-NaYF}_4$ (JCPDS No. 16-0334) and Fe_3O_4 (JCPDS No. 19-0629), as shown in Figure 1C, which suggests that the synthesized MNPs@UCNPs were composed of Fe_3O_4 and $\beta\text{-NaYF}_4$. Figure 1D shows the surface properties of nanoparticles by FTIR spectra. The peak at 573 cm^{-1} and 580 cm^{-1} was the characteristic band of Fe-O, which reflected the appearance of Fe_3O_4 . Before ADA modification, there were three apparent peaks at 1410 cm^{-1} , 1610 cm^{-1} , and 3410 cm^{-1} . The peaks at 1410 cm^{-1} and 1610 cm^{-1} were attributed to the $-\text{COOH}$ groups of OA-coated UCNPs. Furthermore, the band at 3410 cm^{-1} was ascribed to the stretching vibration of hydroxide radicals. After ligand exchange with ADA, the peak of 1040 cm^{-1} appeared, which related to the stretching vibration of P-O of ADA [32,34].

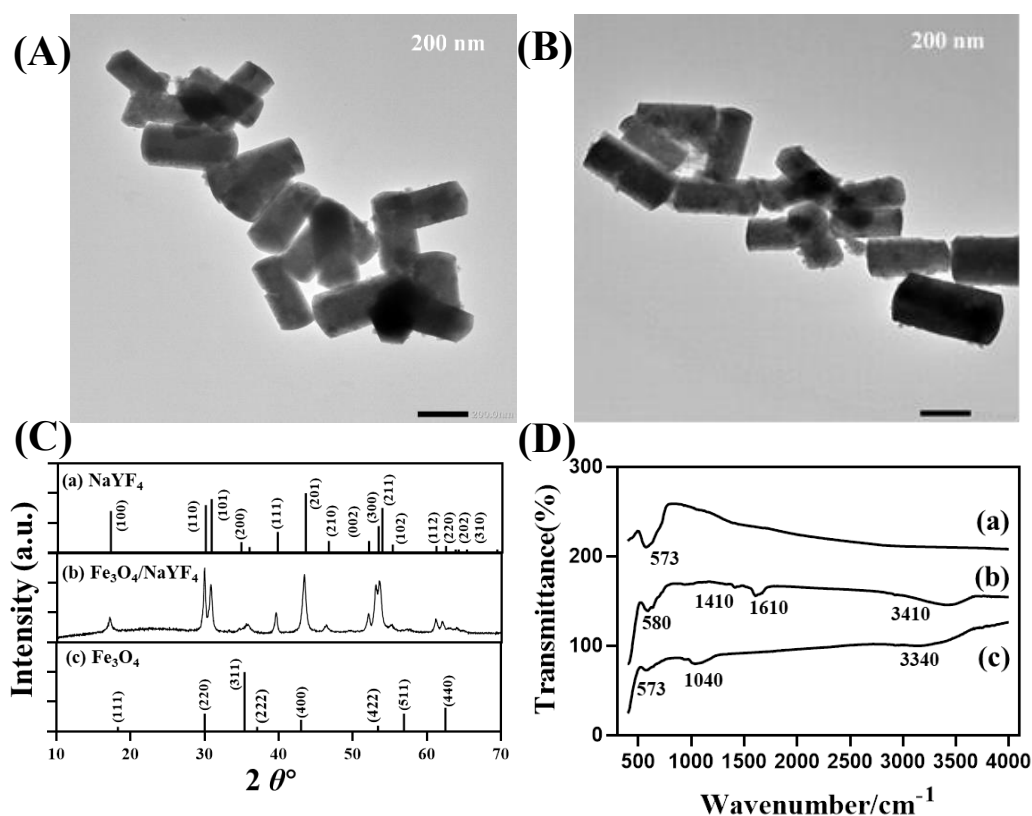


Figure 1. (A) TEM image of Fe_3O_4 NPs@UCNPs before ADA modification; (B) TEM image of Fe_3O_4 NPs@UCNPs after ADA modification; (C) XRD patterns of NaYF_4 , $\text{Fe}_3\text{O}_4/\text{NaYF}_4$, and Fe_3O_4 ; (D) FTIR spectra of Fe_3O_4 (a), $\text{Fe}_3\text{O}_4/\text{NaYF}_4$ (b), and ADA- $\text{Fe}_3\text{O}_4/\text{NaYF}_4$ (c).

3.2. Feasibility for *Shigella* Detection

Based on the inner filter effect between MNPs@UCNPs and oxTMB, the fluorescence biosensor for *Shigella* detection was developed. It was widely known that the spectrum overlapping of fluorescence donor and acceptor was primarily responsible for the mechanism of the inner filter effect. Figure 2A shows that the fluorescence intensity of MNPs@UCNPs significantly decreased when the absorption of oxTMB and the fluorescence spectrum

of MNPs@UCNPs overlapped. In addition, Scheme 1 demonstrates the principle of the proposed method for *Shigella* detection. Firstly, Fe₃O₄ nanoparticles were synthesized by the solvothermal method and simultaneously performed excellent dispersity and magnetic properties. On this basis, MNPs@UCNPs were fabricated via a facile hydrothermal method. Then, the nanoparticles were modified with the complementary strand. Due to base pairing, complementary strand-modified MNPs@UCNPs combined with *Shigella* aptamer-modified HRP. In the presence of *Shigella*, HRP with *Shigella* aptamer could separate from MNPs@UCNPs because of the stronger affinity between *Shigella* and aptamers. After removing the HRP, which was unbound with MNPs@UCNPs via magnetic separation, TMB remained colorless owing to the lack of HRP. In the absence of *Shigella*, HRP bound with MNPs@UCNPs would remain through magnetic separation. In this case, TMB was oxidized from colorless into blue with an absorption decrease ranging from 500 nm to 600 nm, which contributed to fluorescence quenching since the absorption band of oxTMB overlapped with the emission peak of MNPs@UCNPs at 545 nm. Figure 2B shows a significant fluorescence recovery with *Shigella* addition, which confirmed the feasibility of the proposed fluorescence biosensor. This method amplified the response signals through magnetic separation to achieve high performance and a lower detecting limitation; hence, it has a great application value for pathogenic bacteria warning early in food safety.

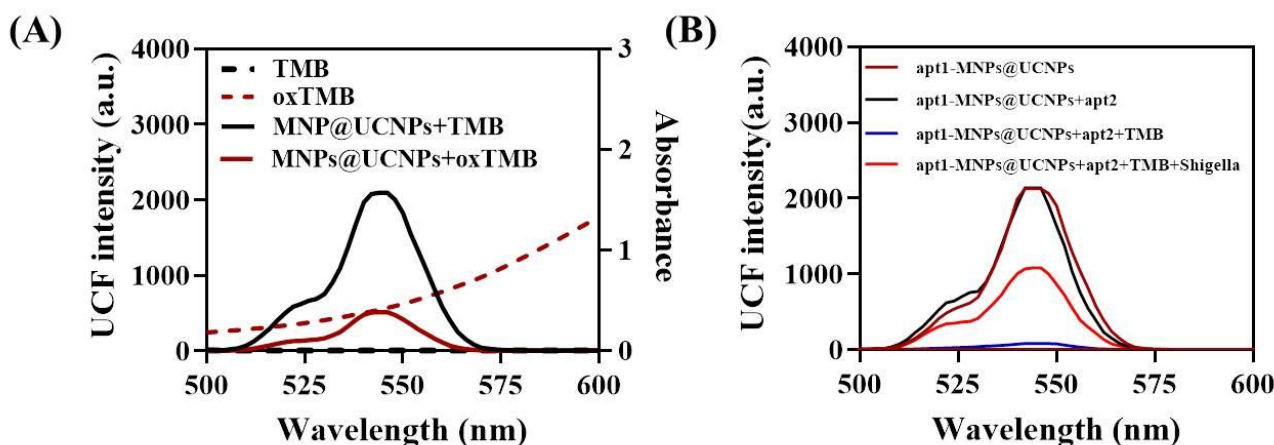


Figure 2. (A) UV-vis absorption spectra of TMB and oxTMB, fluorescence spectra of MNPs@UCNPs + TMB and MNPs@UCNPs + oxTMB; (B) fluorescence spectra of apt1-MNPs@UCNPs, apt1-MNPs@UCNPs-apt2, apt1-MNPs@UCNPs-apt2 + TMB, apt1-MNPs@UCNPs-apt2 + TMB + *Shigella*.

As shown in Figure 3A, there was no significant change between the fluorescence spectrum of different surface modifications onto UCNPs. Meanwhile, Figure 3B shows that MNPs@UCNPs had no effect on TMB oxidation and color change. Based on the above results, the proposed method has convincing stability and feasibility for *Shigella* detection. To confirm that the functionalized MNPs@UCNPs and aptamer conjugate successfully, the UV spectrum of products after incubating was determined, as depicted in Figure 3C. There was a noticeable peak at 280 nm on account of the successful connection of aptamer with MNPs@UCNPs in the mixture of the conjugate.

3.3. Optimization of Experimental Condition

To enhance the sensitivity and efficiency of the proposed sensor, this work optimized several critical factors such as the volume of TMB solution, the concentration of HRP, the response time of TMB and MNPs@UCNPs–HRP conjugates, and the incubation time of *Shigella* and aptamer. Firstly, the sensitivity of the proposed fluorescence biosensor was heavily impacted by the TMB quenching efficiency. Hence, it is necessary to examine the influence of the volume of TMB horseradish peroxidase color development solution on fluorescence quenching. As demonstrated in Figure 4A, the fluorescence intensity gradually decreased with the increase of TMB solution volume. When the volume of the TMB solution

rose to 350 μL , the fluorescence intensity tended to flatten, which proved that 350 μL of TMB solution should be selected for the *Shigella* quantitative analysis. Additionally, the absorption spectra of the TMB and different concentrations of HRP are shown in Figure 4B. The absorption peak tended to stabilize when the concentration of HRP reached 20 $\mu\text{g/L}$. Thus, 20 $\mu\text{g/L}$ was selected as the optimal concentration of HRP. Furthermore, the influence of the response time of TMB oxidization was investigated in Figure 4C. The absorbance increased to about 1.48 and then remained stable at 24 min. Therefore, it is optimal to select 24 min as the final response time. In order to achieve optimal performance, the incubation duration of *Shigella* and aptamer, which has a significant impact on the sensitivity of the proposed fluorescence biosensor, was examined. As shown in Figure 4D, the fluorescence intensity rose continuously and peaked at 23 min. As a result, 23 min was determined to be the ideal incubation time for *Shigella* detection.

3.4. Analytical Performance of the Fluorescence Biosensor for *Shigella* Detection

After optimizing the experimental conditions, the proposed fluorescence biosensor measured different concentrations of *Shigella* by monitoring the emission peaks of the UCNP's fluorescence intensity at 545 nm. In the presence of *Shigella*, HRP with *Shigella* aptamer could separate from MNPs@UCNPs due to the stronger affinity between *Shigella* and aptamers, resulting in an increased fluorescence intensity at 545 nm. In the absence of *Shigella*, HRP with MNPs@UCNPs would remain in solution, and oxidized TMB to blue, contributing to fluorescence quenching at 545 nm based on the inner filter effect, as demonstrated in Figure 5A. As shown in Figure 5B, there was a strong linear correlation between fluorescence intensity and the logarithm of *Shigella* concentrations ($\log C$) ranging from 2.3×10^2 CFU/mL to 2.3×10^7 CFU/mL ($Y = 259.5 \log C - 608.48$, $R^2 = 0.9919$). The limit of detection was calculated to be 32 CFU/mL according to the formula $3S_0/K$ ($3S_0$ is the standard deviation of 11 blank measurements, and K is the slope of the *Shigella* detection calibration plot) [35]. These results confirmed that the MNPs@UCNP's fluorescence sensor had excellent detection performance and potential application in bacteria determination. More importantly, there was a comparison between this work and other methods in Table 1 from the aspects of linear range, the limit of detection, and detection time, which confirmed that the proposed MNPs@UCNP's fluorescence sensor possessed broad prospects in foodborne pathogen monitoring. The proposed fluorescence biosensor has good results in a relatively short time compared with other biosensors [36–38]. To further explore the superiority of the fabricated method, we also made a comparative analysis of this method with other fluorescence biosensors. Unlike other fluorescence sensors shown in Table 1 [39,40], which require incubation with fluorescent probes, the approach we constructed was more straightforward, because the detected system possesses fluorescence emission intensity after magnetic separation.

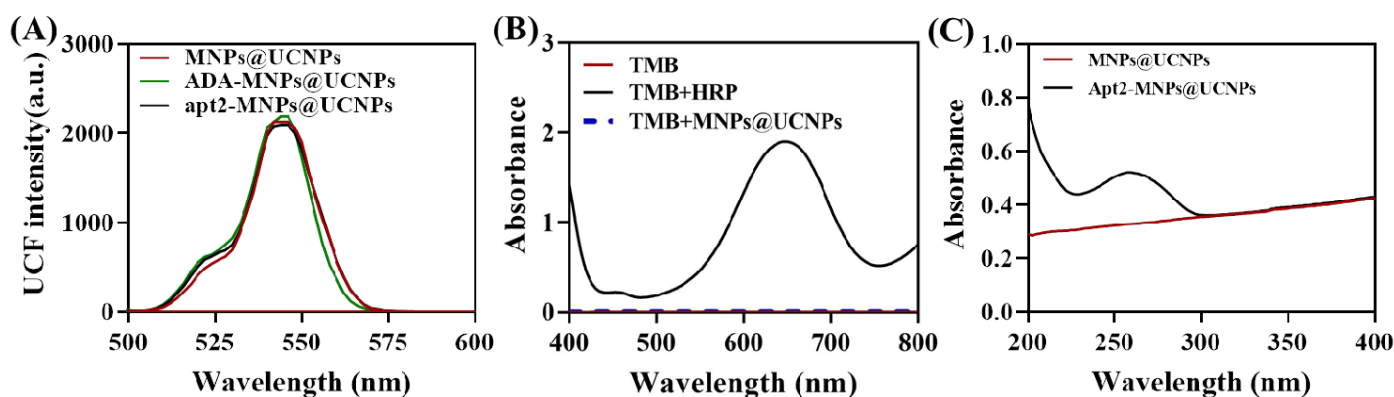


Figure 3. (A) Fluorescence spectra of MNPs@UCNPs, ADA-MNPs@UCNPs, and apt2-MNPs@UCNPs; (B) UV-vis spectra of TMB, TMB + HRP, and TMB + MNPs@UCNPs; (C) UV-vis spectra of MNPs@UCNPs and apt2-MNPs@UCNPs.

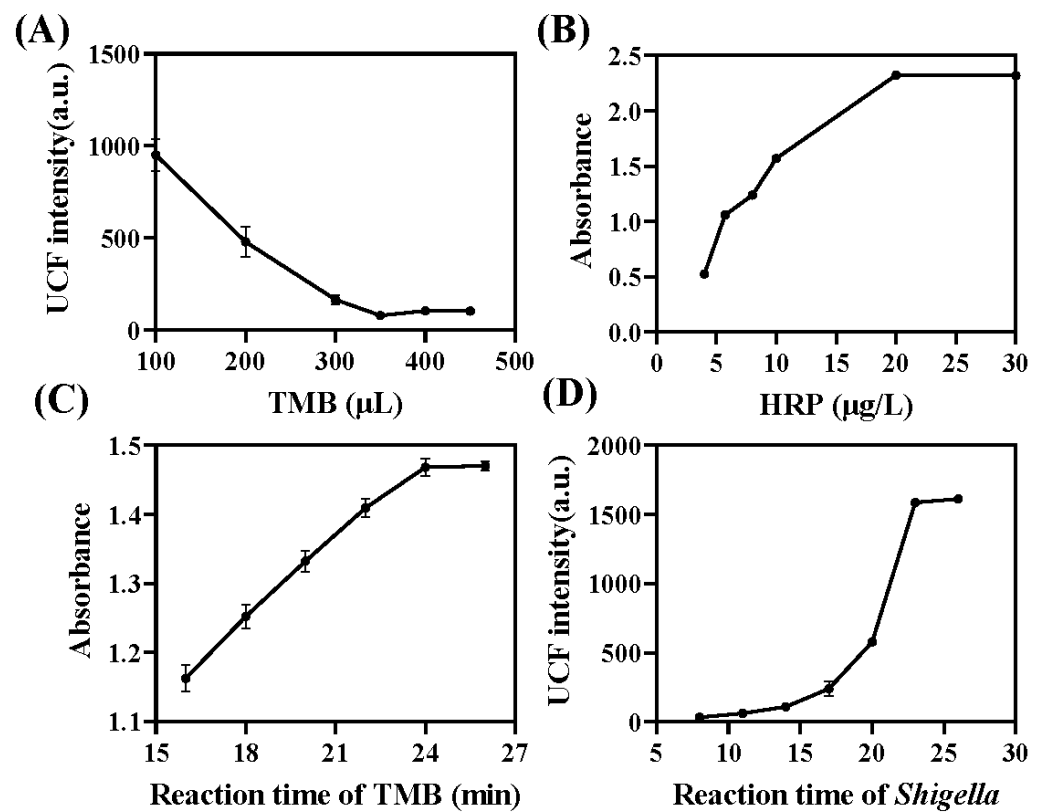


Figure 4. (A) Optimized condition of the volume of TMB; (B) the concentration of HRP; (C) the response time of TMB and MNPs@UCNPs–HRP conjugates; (D) and the incubation time of *Shigella* and aptamer.

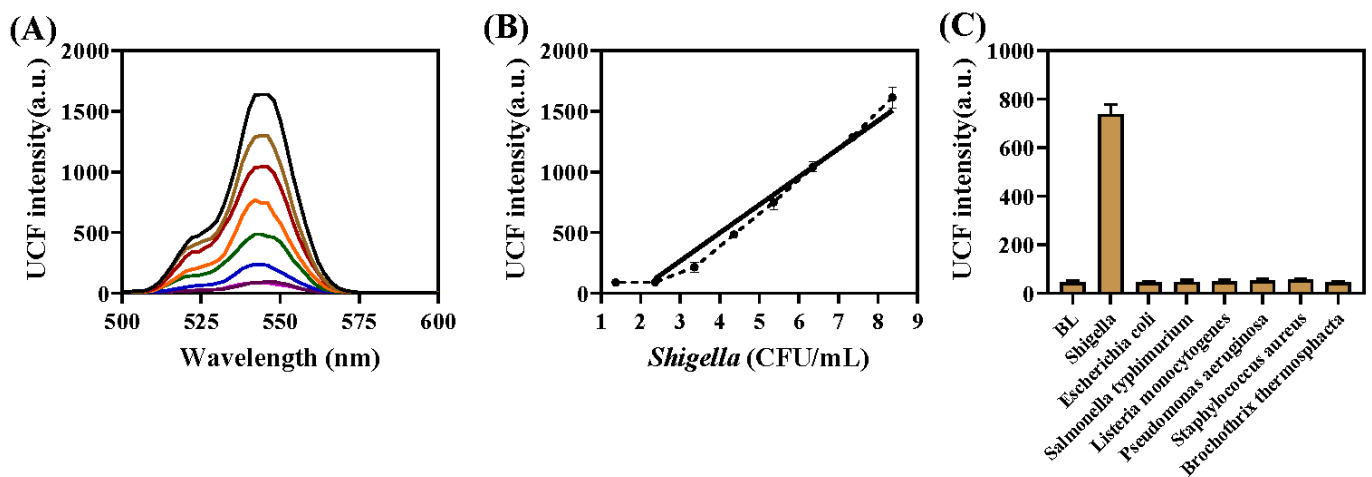


Figure 5. (A) Fluorescence spectra of the proposed method with various *Shigella* concentrations from 2.3×10^7 CFU/mL to 2.3×10^1 CFU/mL; (B) calibration curve of fluorescence intensity at 545 nm of the proposed method with various *Shigella* concentrations; (C) fluorescence intensity of MNPs@UCNPs fluorescence sensor with the addition of different bacteria.

Table 1. Comparison of the sensitivity of this work and other methods for *Shigella* detection.

Method	Linear Range (CFU/mL)	LOD (CFU/mL)	Detection Time	Reference
Electrochemical DNA biosensor	80– 8×10^8	10	1.5 h	[36]
Electrochemical sensor	3×10^3 – 3×10^4	18	78 min	[37]
SERS biosensor	10– 10^6	10	1.5 h	[38]
Fluorescence sensor	10^3 – 10^8	2.5×10^2	1 h	[39]
Fluorescence sensor	10^3 – 10^7	10^3	1.5h	[40]
MNPs@UCNPs fluorescence sensor	2.3×10^2 – 2.3×10^7	32	1 h	This work

3.5. Selectivity for *Shigella* Detection

Selectivity is a crucial factor in evaluating the performance of the developed MNPs@UCNPs fluorescence biosensor, which is also the ability to assess the detection system against interference from nontargets. It was estimated whether the proposed fluorescence biosensor was capable of determining *Shigella* against the potential interferences from other foodborne pathogens. Figure 5C shows the intensity of fluorescence signal of the MNPs@UCNPs fluorescence biosensor after adding the *Shigella* (ATCC 12022) and nontarget bacteria (*Salmonella typhimurium* (ATCC 14028), *Listeria monocytogenes* (ATCC 19111), *Staphylococcus aureus* (ATCC 130), *Pseudomonas aeruginosa* (ATCC 27853), *Escherichia coli* (ATCC 43889), and *Streptococcus thermophile* (ATCC 03872)). It is obvious that the detection system has a significant fluorescence change only in the presence of the *Shigella* based on the specific recognition between *Shigella* and aptamer, which verified that the MNPs@UCNPs fluorescence biosensor had good selectivity towards *Shigella* detection.

3.6. Detection of *Shigella* in Spiked Chicken Sample

The MNPs@UCNPs fluorescence biosensor was applied to chicken samples analysis with different concentrations of *Shigella* to validate the potential application. Plate counting, which is regarded as the conventional detecting method, was used to analyze the spiked chicken samples. As shown in Table 2, the developed MNPs@UCNPs fluorescence biosensor exhibited excellent recoveries from 97.8% to 108.5%, which had no significant difference from the plate counting method. Although the *Shigella* was spiked into chicken samples, the results acted with little interference with the quantitative assay. It may be caused by MNPs separating the target from the food matrix, which performs high potential applications in foodborne pathogens monitoring.

Table 2. Determination of *Shigella* in chicken samples by the proposed method.

Sample	Spiked Levels (CFU/mL)	Measured (Mean \pm SD) (CFU/mL)		Recovery (%)
		This Work	Plate Count	
Chicken	10^3	$(1.034 \pm 0.130) \times 10^3$	$(1.025 \pm 0.071) \times 10^3$	103.4
	10^3	$(1.065 \pm 0.084) \times 10^3$	$(1.011 \pm 0.124) \times 10^3$	106.5
	10^3	$(0.892 \pm 0.191) \times 10^3$	$(0.914 \pm 0.218) \times 10^3$	106.5
	10^4	$(1.085 \pm 0.122) \times 10^4$	$(1.064 \pm 0.131) \times 10^4$	108.5
	10^4	$(1.042 \pm 0.108) \times 10^4$	$(1.107 \pm 0.151) \times 10^4$	104.2
	10^4	$(0.986 \pm 0.130) \times 10^4$	$(0.951 \pm 0.087) \times 10^4$	98.6
	10^5	$(0.978 \pm 0.240) \times 10^5$	$(1.013 \pm 0.111) \times 10^5$	97.8
	10^5	$(1.074 \pm 0.070) \times 10^5$	$(1.012 \pm 0.108) \times 10^5$	107.4
	10^5	$(1.064 \pm 0.267) \times 10^5$	$(0.997 \pm 0.121) \times 10^5$	106.4

4. Conclusions

In summary, a novel and sensitive nanoplatfrom based on biofunctionalized MNPs@UCNPs as the fluorescence donor and oxTMB as the fluorescence acceptor was fabricated to detect *Shigella* quantitatively. The fluorescence signal of UCNPs at 545 nm was quenched by

oxTMB based on the inner filter effect in the absence of *Shigella* and recovered due to the strong affinity between *Shigella* and aptamer in the presence of *Shigella*. On the basis of the above changes, the concentrations of *Shigella* were quantified by the change of the fluorescence intensity ranging from 2.3×10^2 to 2.3×10^7 CFU/mL with a LOD of 32 CFU/mL. Furthermore, the proposed fluorescence biosensor acted with an excellent result for sensitivity, specificity, stability, as well applicability, confirming that the developed method had a broad prospect in foodborne pathogens detection and food safety monitoring.

Author Contributions: Y.S. and M.C.: investigation, methodology, and writing—original draft; Z.Y.: methodology, formal analysis, and resources; L.H.: software and writing—original draft; L.P.: conceptualization, methodology, and funding acquisition; K.T.: supervision, project administration, and funding acquisition. All authors have read and agreed to the published version of the manuscript.

Funding: This work was supported by the Jiangsu Provincial Key Research and Development Program (BE2021719 and BE2020693), the Jiangsu Province Graduate Research and Innovation Program (KYCX21_0578), the Science and Technology Project of Jiangsu Provincial Market Supervision Administration (KJ2023066), the Natural Science Research Plan of Huai'an (HAB202243), and the National Key R&D Program of China (2022YFF1100801).

Institutional Review Board Statement: Not applicable.

Informed Consent Statement: Not applicable.

Data Availability Statement: Not applicable.

Conflicts of Interest: The authors declare no conflict of interest.

References

1. Li, H.; Ahmad, W.; Rong, Y.; Chen, Q.; Zuo, M.; Ouyang, Q.; Guo, Z. Designing an Aptamer Based Magnetic and Upconversion Nanoparticles Conjugated Fluorescence Sensor for Screening Escherichia Coli in Food. *Food Control*. **2020**, *107*, 106761. [[CrossRef](#)]
2. Bintsis, T. Foodborne Pathogens. *AIMS Microbiol.* **2017**, *3*, 529–563. [[CrossRef](#)]
3. He, P.; Wang, H.; Yan, Y.; Zhu, G.; Chen, Z. Development and Application of a Multiplex Fluorescent PCR for Shigella Detection and Species Identification. *J. Fluoresc.* **2022**, *32*, 707–713. [[CrossRef](#)] [[PubMed](#)]
4. Li, Y.; Chen, M.; Fan, X.; Peng, J.; Pan, L.; Tu, K.; Chen, Y. Sandwich Fluorometric Method for Dual-Role Recognition of Listeria Monocytogenes Based on Antibiotic-Affinity Strategy and Fluorescence Quenching Effect. *Anal. Chim. Acta* **2022**, *1221*, 340085. [[CrossRef](#)] [[PubMed](#)]
5. Rajapaksha, P.; Elbourne, A.; Gangadoo, S.; Brown, R.; Cozzolino, D.; Chapman, J. A Review of Methods for the Detection of Pathogenic Microorganisms. *Analyst* **2019**, *144*, 396–411. [[CrossRef](#)] [[PubMed](#)]
6. Zhao, Y.; Chen, F.; Li, Q.; Wang, L.; Fan, C. Isothermal Amplification of Nucleic Acids. *Chem. Rev.* **2015**, *115*, 12491–12545. [[CrossRef](#)]
7. Wu, Y.; Choi, N.; Chen, H.; Dang, H.; Chen, L.; Choo, J. Performance Evaluation of Surface-Enhanced Raman Scattering-Polymerase Chain Reaction Sensors for Future Use in Sensitive Genetic Assays. *Anal. Chem.* **2020**, *92*, 2628–2634. [[CrossRef](#)]
8. Hosseini, S.; Vázquez-Villegas, P.; Rito-Palomares, M.; Martínez-Chapa, S.O. Advantages, Disadvantages and Modifications of Conventional ELISA. In *Enzyme-Linked Immunosorbent Assay (ELISA)*; Springer: Singapore, 2018; pp. 67–115. [[CrossRef](#)]
9. Yu, H.; Guo, W.; Lu, X.; Xu, H.; Yang, Q.; Tan, J.; Zhang, W. Reduced Graphene Oxide Nanocomposite Based Electrochemical Biosensors for Monitoring Foodborne Pathogenic Bacteria: A Review. *Food Control*. **2021**, *127*, 108117. [[CrossRef](#)]
10. Li, C.-C.; Wang, Z.-Y.; Wang, L.-J.; Zhang, C.-Y. Biosensors for Epigenetic Biomarkers Detection: A Review. *Biosens. Bioelectron.* **2019**, *144*, 111695. [[CrossRef](#)]
11. Park, S.-H.; Kwon, N.; Lee, J.-H.; Yoon, J.; Shin, I. Synthetic Ratiometric Fluorescent Probes for Detection of Ions. *Chem. Soc. Rev.* **2020**, *49*, 143–179. [[CrossRef](#)]
12. Li, Q.; Chen, P.; Wang, J.; Zhang, S.; Yan, J. Detection of Salmonella, Shigella and Staphylococcus aureus based on quantum dots and immunomagnetic beads. *Wei Sheng Yan Jiu* **2013**, *42*, 660–663.
13. Zhang, J.; Zhou, M.; Li, X.; Fan, Y.; Li, J.; Lu, K.; Wen, H.; Ren, J. Recent Advances of Fluorescent Sensors for Bacteria Detection-A Review. *Talanta* **2023**, *254*, 124133. [[CrossRef](#)]
14. Yao, Y.; Xie, G.; Zhang, X.; Yuan, J.; Hou, Y.; Chen, H. Fast Detection of E. Coli with a Novel Fluorescent Biosensor Based on a FRET System between UCNPs and GO@Fe₃O₄ in Urine Specimens. *Anal. Methods* **2021**, *13*, 2209–2214. [[CrossRef](#)]
15. Wang, P.; Wang, A.; Hassan, M.M.; Ouyang, Q.; Li, H.; Chen, Q. A Highly Sensitive Upconversion Nanoparticles-WS₂ Nanosheet Sensing Platform for Escherichia Coli Detection. *Sens. Actuators B Chem.* **2020**, *320*, 128434. [[CrossRef](#)]
16. Abdul Hakeem, D.; Su, S.; Mo, Z.; Wen, H. Upconversion Luminescent Nanomaterials: A Promising New Platform for Food Safety Analysis. *Crit. Rev. Food Sci. Nutr.* **2022**, *62*, 8866–8907. [[CrossRef](#)] [[PubMed](#)]

17. Selva Sharma, A.; Marimuthu, M.; Varghese, A.W.; Wu, J.; Xu, J.; Xiaofeng, L.; Devaraj, S.; Lan, Y.; Li, H.; Chen, Q. A Review of Biomolecules Conjugated Lanthanide Up-Conversion Nanoparticles-Based Fluorescence Probes in Food Safety and Quality Monitoring Applications. *Crit. Rev. Food Sci. Nutr.* **2023**, 1–31. [[CrossRef](#)]
18. Huang, Z.; Liu, Y.; Chen, Y.; Xiong, Q.; Wang, Y.; Duan, H.; Lai, W. Improving the Performance of Upconversion Nanoprobe-Based Lateral Flow Immunoassays by Supramolecular Self-Assembly Core/Shell Strategies. *Sens. Actuators B Chem.* **2020**, *318*, 128233. [[CrossRef](#)]
19. Wen, Z.; Hu, X.; Yan, R.; Wang, W.; Meng, H.; Song, Y.; Wang, S.; Wang, X.; Tang, Y. A Reliable Upconversion Nanoparticle-Based Immunochromatographic Assay for the Highly Sensitive Determination of Olaquinox in Fish Muscle and Water Samples. *Food Chem.* **2023**, *406*, 135081. [[CrossRef](#)]
20. Chen, M.; Yan, Z.; Han, L.; Zhou, D.; Wang, Y.; Pan, L.; Tu, K. Upconversion Fluorescence Nanoprobe-Based FRET for the Sensitive Determination of Shigella. *Biosensors* **2022**, *12*, 795. [[CrossRef](#)] [[PubMed](#)]
21. Ouyang, Q.; Wang, L.; Ahmad, W.; Rong, Y.; Li, H.; Hu, Y.; Chen, Q. A Highly Sensitive Detection of Carbendazim Pesticide in Food Based on the Upconversion-MnO₂ Luminescent Resonance Energy Transfer Biosensor. *Food Chem.* **2021**, *349*, 129157. [[CrossRef](#)]
22. Shao, H.; Ma, Q.; Yu, W.; Dong, X.; Hong, X. “Off-On” Typed Upconversion Fluorescence Resonance Energy Transfer Probe for the Determination of Cu²⁺ in Tap Water. *Spectrochim. Acta Part. A Mol. Biomol. Spectrosc.* **2022**, *271*, 120920. [[CrossRef](#)]
23. Xu, J.; Liu, R.; Li, H.; Chen, Q. Multifunctional Upconversion Nanoparticles Based LRET Aptasensor for Specific Detection of As(III) in Aquatic Products. *Sens. Actuators B Chem.* **2022**, *369*, 132271. [[CrossRef](#)]
24. Xiao, F.; Li, W.; Xu, H. Advances in Magnetic Nanoparticles for the Separation of Foodborne Pathogens: Recognition, Separation Strategy, and Application. *Compr. Rev. Food Sci. Food Saf.* **2022**, *21*, 4478–4504. [[CrossRef](#)]
25. Ouyang, Q.; Liu, Y.; Chen, Q.; Guo, Z.; Zhao, J.; Li, H.; Hu, W. Rapid and Specific Sensing of Tetracycline in Food Using a Novel Upconversion Aptasensor. *Food Control* **2017**, *81*, 156–163. [[CrossRef](#)]
26. Elahi, N.; Kamali, M.; Baghersad, M.H.; Amini, B. A Fluorescence Nano-Biosensors Immobilization on Iron (MNPs) and Gold (AuNPs) Nanoparticles for Detection of Shigella spp. *Mater. Sci. Eng. C* **2019**, *105*, 110113. [[CrossRef](#)] [[PubMed](#)]
27. Shi, X.; Sun, H.; Li, H.; Wei, S.; Jin, J.; Zhao, C.; Wang, J.; Li, H. Preparation of IgY Oriented Conjugated Fe₃O₄ MNPs as Immunomagnetic Nanoprobe for Increasing Enrichment Efficiency of Staphylococcus Aureus Based on Adjusting the PH of the Solution System. *Front. Public Health* **2022**, *10*, 865828. [[CrossRef](#)] [[PubMed](#)]
28. Feng, J.; Shen, Q.; Wu, J.; Dai, Z.; Wang, Y. Naked-Eyes Detection of Shigella Flexneri in Food Samples Based on a Novel Gold Nanoparticle-Based Colorimetric Aptasensor. *Food Control* **2019**, *98*, 333–341. [[CrossRef](#)]
29. Si, S.; Li, C.; Wang, X.; Yu, D.; Peng, Q.; Li, Y. Magnetic Monodisperse Fe₃O₄ Nanoparticles. *Cryst. Growth Des.* **2005**, *5*, 391–393. [[CrossRef](#)]
30. Liu, D.; Zhao, D.; Shi, F.; Zheng, K.; Qin, W. Superparamagnetic and Upconversion Luminescent Properties of Fe₃O₄/NaYF₄:Yb, Er Hetero-Submicro-Rods. *Mater. Lett.* **2012**, *85*, 1–3. [[CrossRef](#)]
31. Chen, M.; Pan, L.; Tu, K. A Fluorescence Biosensor for Salmonella Typhimurium Detection in Food Based on the Nano-Self-Assembly of Alendronic Acid Modified Upconversion and Gold Nanoparticles. *Anal. Methods* **2021**, *13*, 2415–2423. [[CrossRef](#)]
32. Chen, M.; Hassan, M.; Li, H.; Chen, Q. Fluorometric Determination of Lead(II) by Using Aptamer-Functionalized Upconversion Nanoparticles and Magnetite-Modified Gold Nanoparticles. *Microchim. Acta* **2020**, *187*, 85. [[CrossRef](#)] [[PubMed](#)]
33. Jung, T.; Jung, Y.; Ahn, J.; Yang, S. Continuous, Rapid Concentration of Foodborne Bacteria (Staphylococcus Aureus, Salmonella Typhimurium, and Listeria Monocytogenes) Using Magnetophoresis-Based Microfluidic Device. *Food Control* **2020**, *114*, 107229. [[CrossRef](#)]
34. Zhang, Y.; Zhang, Y.; Zhang, X.; Li, Y.; He, Y.; Liu, Y.; Ju, H. A Photo Zipper Locked DNA Nanomachine with an Internal Standard for Precise MiRNA Imaging in Living Cells. *Chem. Sci.* **2020**, *11*, 6289–6296. [[CrossRef](#)]
35. Wang, W.; Zhang, Y.; Zhang, W.; Liu, Y.; Ma, P.; Wang, X.; Sun, Y.; Song, D. A Novel Sensing Platform for the Determination of Alkaline Phosphatase Based on SERS-Fluorescent Dual-Mode Signals. *Anal. Chim. Acta* **2021**, *1183*, 338989. [[CrossRef](#)] [[PubMed](#)]
36. Ali, M.R.; Bacchu, M.S.; Das, S.; Akter, S.; Rahman, M.M.; Saad Aly, M.A.; Khan, M.Z.H. Label Free Flexible Electrochemical DNA Biosensor for Selective Detection of Shigella Flexneri in Real Food Samples. *Talanta* **2023**, *253*, 123909. [[CrossRef](#)] [[PubMed](#)]
37. Luo, J.; Wang, J.; Mathew, A.S.; Yau, S.-T. Ultrasensitive Detection of Shigella Species in Blood and Stool. *Anal. Chem.* **2016**, *88*, 2010–2014. [[CrossRef](#)]
38. Wu, S.; Duan, N.; He, C.; Yu, Q.; Dai, S.; Wang, Z. Surface-Enhanced Raman Spectroscopic-Based Aptasensor for Shigella Sonnei Using a Dual-Functional Metal Complex-Ligated Gold Nanoparticles Dimer. *Colloids Surf. B Biointerfaces* **2020**, *190*, 110940. [[CrossRef](#)] [[PubMed](#)]
39. Yin, M.; Wu, C.; Li, H.; Jia, Z.; Deng, Q.; Wang, S.; Zhang, Y. Simultaneous Sensing of Seven Pathogenic Bacteria by Guanidine-Functionalized Upconversion Fluorescent Nanoparticles. *ACS Omega* **2019**, *4*, 8953–8959. [[CrossRef](#)]
40. Song, M.-S.; Sekhon, S.S.; Shin, W.-R.; Kim, H.C.; Min, J.; Ahn, J.-Y.; Kim, Y.-H. Detecting and Discriminating Shigella Sonnei Using an Aptamer-Based Fluorescent Biosensor Platform. *Molecules* **2017**, *22*, 825. [[CrossRef](#)]

Disclaimer/Publisher’s Note: The statements, opinions and data contained in all publications are solely those of the individual author(s) and contributor(s) and not of MDPI and/or the editor(s). MDPI and/or the editor(s) disclaim responsibility for any injury to people or property resulting from any ideas, methods, instructions or products referred to in the content.